

Single-Pixel Compressive Imaging in Shift-Invariant Spaces via Exact Wavelet Frames

Tin Vlašić and Damir Seršić

Abstract

This paper introduces a novel framework for single-pixel imaging via compressive sensing (CS) in shift-invariant (SI) spaces by exploiting the sparsity property of a wavelet representation. We reinterpret the acquisition procedure of a single-pixel camera as filtering of the observed signal with continuous-domain functions that lie in an SI subspace spanned by the integer shifts of the box function. The signal is modeled by an arbitrary SI generator whose special case is the box function, which, as we show in the paper, is conventionally used in single-pixel imaging. We propose to use separable B-spline generators which are intuitively complemented by sparsity-inducing spline wavelets. The SI models of the acquisition and the underlying signal lead to an exact discretization of an inherently continuous-domain inverse problem to a finite-dimensional problem of CS type. By solving the CS optimization problem, a parametric representation of the signal is obtained. Such a representation offers many practical advantages in image processing applications. We propose an efficient matrix-free implementation of the framework and conduct it on the standard test images and real-world measurement data. Experimental results show that the proposed framework achieves a significant improvement of the reconstruction quality relative to the conventional CS setting.

Index Terms

This research was supported in part by the European Regional Development Fund under the grant KK.01.1.1.01.0009 (DATACROSS) and in part by the Croatian Science Foundation under the project IP-2019-04-6703.

T. Vlašić and D. Seršić are with the Department of Electronic Systems and Information Processing, University of Zagreb Faculty of Electrical Engineering and Computing, Unska 3, HR-10000 Zagreb, Croatia (e-mail: tin.vlasic@fer.hr; damir.sersic@fer.hr).

This work has been submitted to the IEEE for possible publication. Copyright may be transferred without notice, after which this version may no longer be accessible.

Compressed sensing, discrete wavelet transform, image reconstruction, image sampling, inverse problems, splines

I. INTRODUCTION

Sampling theories are concerned with the reconstruction of analog signals from discrete-time samples. Being an ill-posed inverse problem, reconstruction from samples must rely on some signal prior, e.g., an assumption that the observed signal lies in a predefined subspace. In conventional sampling, famously embodied in the Nyquist-Shannon theorem [1], [2], signals are assumed to lie in a shift-invariant (SI) subspace spanned by the integer shifts of the sinc function, where $\text{sinc}(t) = \sin(\pi t)/(\pi t)$. The Nyquist-Shannon theorem was generalized to a wider class of SI subspaces [3]–[5], which allows more realistic sampling schemes and signal representations, including splines [6] and wavelets [7], [8]. To obtain an exact reconstruction, the signal has to be sampled at least at the rate of innovation [9], which corresponds to the Nyquist limit in the conventional sampling theorem.

During the past two decades, sparsity has become an important signal prior in the field of signal processing. It lies at the heart of compressive sensing (CS) [10]–[12], a sampling and reconstruction method that goes beyond the Nyquist limit. In standard CS, an unknown signal $f : D \rightarrow \mathbb{R}$, where D is an uncountable subset of \mathbb{R} in a region of interest, is assumed to be exactly represented as the linear combination $\sum_{n=1}^N x_n \xi_n$ of a finite number of basis functions. The coefficients $\{x_n\}_{n=1}^N$ are a discrete-time representation of the observed continuous-domain signal and are assumed to be Q -sparse, where $Q \ll N$. The measurement procedure is described by a linear operator \mathbf{z} , which yields discrete samples $\mathbf{y} = \mathbf{z}(f) \in \mathbb{R}^M$, where $2Q \lesssim M < N$. Signal reconstruction is then given by the optimization problem

$$\arg \min_{\mathbf{x} \in \mathbb{R}^N} \|\mathbf{y} - \mathbf{\Theta} \mathbf{x}\|_{\ell_2}^2 + \lambda \|\mathbf{x}\|_{\ell_1}, \quad (1)$$

where $\mathbf{\Theta} : \mathbb{R}^N \rightarrow \mathbb{R}^M$ is a discrete version of the forward model, with elements $[\mathbf{\Theta}]_{m,n} = \langle z_m, \xi_n \rangle$. While the ℓ_2 -norm is used to measure the consistency of the solution with the measurements, the ℓ_1 -norm regularization promotes sparse solutions.

In the vast majority of papers, the discrete version of a continuous-domain forward model is an approximation that introduces errors to real-world implementations of CS acquisition systems. Furthermore, one typically assumes the bandlimited model of the underlying signal, which may additionally contribute to the reconstruction error if its continuous-domain generator is not considered in the discretization procedure. There have been several attempts to generalize CS to infinite-dimensional problems, that were reported in [13]–[15]. The SI signal model is employed in a few works to exactly discretize continuous-domain inverse problems into CS-type problems. In [16] and [17], Eldar and Mishali use CS for reconstruction of

signals in unions of SI subspaces. Sparsity is modeled by assuming that only a few out of all generators in the union are active. The authors of [18]–[20] use splines as a representation basis of the underlying signal for the discretization of the continuous-domain inverse problems. The signal is assumed to be sparse in the representation basis, i.e. it has only a few innovations per time unit. A different approach is considered in [21] and [22], where an SI model of the underlying one-dimensional signal is used to exactly discretize an inherently continuous-domain inverse problem, and the expansion coefficients of the SI model are assumed to be sparse in a certain discrete transform domain.

In this paper, we propose to use SI models for the discretization of the underlying signal and the acquisition procedure in single-pixel imaging. The concept of a single-pixel camera followed the birth of the CS theory and was first reported by Duarte et al. in [23]. Over the past decade, single-pixel imaging has been used in many applications and has several areas of possible advantage [24]. A single-pixel camera consists of two components - the light modulator and the single-pixel detector. The light modulator is usually implemented by the digital micromirror device (DMD), which selectively redirects the light beams to the photodetector or projects the sequence of light patterns onto the object that is being captured by the detector. We model the DMD modulation procedure with two-dimensional filtering by separable functions that lie in an SI subspace spanned by the box function, which is also referred to as the B-spline of order 0. The underlying signal is assumed to lie in an arbitrary SI subspace. We link the theories of generalized sampling in SI spaces and CS to discretize the inherently continuous-domain inverse problem of single-pixel imaging exactly. We propose to use polynomial B-splines as a representation basis of the signal. The polynomial B-splines are compactly supported and provide many practical advantages in image processing once their expansion coefficients are recovered directly from a reduced set of measurements. We employ spline wavelets as sparsity-inducing bases, which offer an intuitive complement of the B-spline function spaces. We show that when the B-spline representation function corresponds to the wavelet scaling function, the recovered wavelet coefficients exactly match the orthogonal projection of the underlying signal onto the continuous-domain analysis wavelet functions. We offer an efficient matrix-free implementation of the proposed framework which significantly reduces the computational costs of the reconstruction algorithm and suits the application to large-scale images. The reconstruction quality of the framework was assessed on the standard test images and data acquired by an off-the-shelf realization of the single-pixel camera. Experimental results show that the proposed framework improves the reconstruction quality relative to the conventional single-pixel imaging framework.

The paper is organized as follows: we give a short reminder on multiresolution representation in Section II, with the emphasis placed on the orthogonal projection of signals onto the Riesz bases. In Section III, we link multiresolution representation with the generalized sampling in SI spaces and extend the

results to higher dimensions in Section IV. In Section V, we propose a novel framework for single-pixel imaging via CS in SI spaces based on a wavelet-domain sparsity assumption. In Section VI, an efficient implementation of the proposed framework for large-scale images is suggested. Experimental results are illustrated in Section VII. We relate our work to the findings of other studies in Section VIII and conclude the paper in Section IX.

II. MULTIREOLUTION REPRESENTATION

We deal with the problem of recovering and representing an unknown function $f(t)$ that lies in the Hilbert space L_2 , which consists of functions that are square-integrable and whose inner product is defined by

$$\langle f(t), g(t) \rangle = \int_{-\infty}^{\infty} f^*(t)g(t)dt, \quad (2)$$

for some $g(t) \in L_2$. In order to recover $f(t)$ from its uniform samples, it is commonly assumed that $f(t)$ lies in an appropriate SI subspace $\mathcal{V}_{(0)}$ of L_2 [1]–[5]. Any signal $f(t) \in \mathcal{V}_{(0)}$ has the form

$$f(t) = \sum_{k \in \mathbb{Z}} a_{(0)}[k]\varphi(t - kT), \quad (3)$$

for some generator $\varphi(t)$ and sampling period T . For simplicity, throughout the manuscript, we assume $T = 1$.

To guarantee a unique and stable representation of any signal in $\mathcal{V}_{(0)}$ by expansion coefficients $a_{(0)}[k]$, the generator should form a Riesz basis for L_2 [4], [5]. A countable set of vectors $\{\varphi(t - k)\}$ in L_2 is a Riesz basis for L_2 if it is complete and if and only if there exist two positive constants $\alpha > 0$ and $\beta < \infty$ such that

$$\alpha \|\mathbf{a}_{(0)}\|_{\ell_2}^2 \leq \left\| \sum_{k \in \mathbb{Z}} a_{(0)}[k]\varphi(t - k) \right\|_{L_2}^2 \leq \beta \|\mathbf{a}_{(0)}\|_{\ell_2}^2, \quad (4)$$

where $\|\mathbf{a}_{(0)}\|_{\ell_2}^2 = \sum_k |a_{(0)}[k]|^2$ is the squared ℓ_2 -norm of the expansion coefficients $a_{(0)}[k]$. Namely, a Riesz basis is a set of linearly independent vectors which ensures that a small modification of the expansion coefficients results in a small distortion of the signal representation. In particular, the basis is orthonormal if and only if $\alpha = \beta = 1$. Notice that a set $\{\varphi(t - k)\}$ in L_2 is an exact frame for L_2 if it is a Riesz basis for L_2 [25].

Furthermore, we assume that $\mathcal{V}_{(0)}$ is a subspace in a sequence of nested subspaces such that $\mathcal{V}_{(i)} \supset \mathcal{V}_{(i+1)}$ for $i \in \mathbb{Z}$. These subspaces are spanned by a set of basis vectors $\{\varphi(2^{-i}t - k)\}$, obtained by dilation and

translation of a generator $\varphi(t)$ [7], [8], which is also referred to as a scaling function. Approximation of $f(t) \in L_2$ at resolution 2^i in $\mathcal{V}_{(i)}$ is defined by

$$\hat{f}_{(i)}(t) = \sum_{k \in \mathbb{Z}} a_{(i)}[k] \varphi(2^{-i}t - k). \quad (5)$$

A procedure for obtaining the minimum squared error approximation of a signal $f(t)$ in $\mathcal{V}_{(i)}$ is given below.

The expansion coefficients in (5) of the orthogonal projection of a signal $f(t) \in L_2$ on $\mathcal{V}_{(i)}$ can be determined by filtering and sampling, written in an inner product notation as

$$a_{(i)}[k] = 2^{-i} \langle f(t), \hat{\varphi}(2^{-i}t - k) \rangle, \quad (6)$$

where $\hat{\varphi}(t)$ is a dual function of $\varphi(t)$. Since $\{\varphi(2^{-i}t - k)\}$ is a Riesz basis for L_2 , there is a collection $\{\hat{\varphi}(2^{-i}t - k)\}$ such that $\{\hat{\varphi}(2^{-i}t - k)\}$ is biorthogonal to $\{\varphi(2^{-i}t - k)\}$, i.e.,

$$\langle \varphi(2^{-i}t - k), \hat{\varphi}(2^{-i}t - l) \rangle = 2^i \delta[k - l]. \quad (7)$$

If $\{\varphi(2^{-i}t - k)\}$ is a Riesz basis, then so is its biorthogonal basis [25]. When the set of vectors $\{\varphi(2^{-i}t - k)\}$ spans only a subspace $\mathcal{V}_{(i)} \in L_2$, there may be many choices of a biorthogonal basis in L_2 satisfying (7).

The fact that the subspaces $\mathcal{V}_{(i)}$ are nested implies that the basis vectors $\{\varphi(2^{-i}t - k)\}$ at coarser levels are included in the finer resolution subspaces. Hence, the expansion coefficients $a_{(i+1)}[k]$ can be obtained by discrete-time filtering of $a_{(i)}[k]$ and downsampling by a factor of two [7], [26]. Consequently, all the coefficients $a_{(i)}[k]$ for $i > 0$ can be computed from $a_{(0)}[k]$ by repeating this procedure. Such a sequence of fine-to-coarse approximations defines a multiresolution analysis, called a pyramid transform.

In order to have a complete and reversible multiresolution representation, we have to extract and save the loss of information between the approximation of $f(t)$ at two successive resolutions 2^i and 2^{i+1} . This difference of information is called the detail signal at level 2^{i+1} , and we can denote it by $g_{(i+1)} := \hat{f}_{(i)} - \hat{f}_{(i+1)}$. The detail signal $g_{(i+1)}$ is included in $\mathcal{V}_{(i)}$, and is perpendicular to $\mathcal{V}_{(i+1)}$, i.e., it is given by the orthogonal projection of the signal $f(t)$ on the orthogonal complement of $\mathcal{V}_{(i+1)}$ in $\mathcal{V}_{(i)}$ [7]. Let $\mathcal{W}_{(i+1)}$ be the detail subspace at resolution 2^{i+1} , then $g_{(i+1)} \in \mathcal{W}_{(i+1)}$, $\mathcal{W}_{(i+1)} \perp \mathcal{V}_{(i+1)}$ and $\mathcal{W}_{(i+1)} \oplus \mathcal{V}_{(i+1)} = \mathcal{V}_{(i)}$. In essence, we want to construct sets of SI bases for the sequence of detail subspaces $\{\mathcal{W}_{(i)}, i \in \mathbb{Z}\}$ so that

$$\mathcal{V}_{(i)} = \mathcal{V}_{(I)} \oplus \left(\bigoplus_{j=i+1}^I \mathcal{W}_{(j)} \right), \quad I > i \quad (8)$$

and

$$\mathcal{W}_{(i)} \perp \mathcal{W}_{(j)}, \quad i \neq j. \quad (9)$$

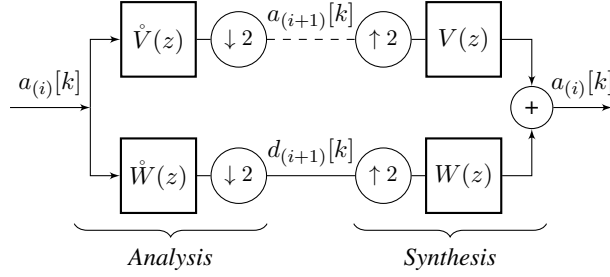


Fig. 1. Filter bank for the forward and inverse wavelet transform.

These subspaces are spanned by basis vectors $\{\psi(2^{-i}t - k)\}$, obtained by dilation and translation of a generator $\psi(t)$ [7], which is also referred to as a mother wavelet.

The detail signal of a function $f(t) \in L_2$ at resolution 2^i has the form

$$g_{(i)}(t) = \sum_{k \in \mathbb{Z}} d_{(i)}[k] \psi(2^{-i}t - k), \quad (10)$$

where $d_{(i)}[k]$ are wavelet coefficients. In order to compute the wavelet coefficients, we can apply the same procedure for obtaining the approximation coefficients $a_{(i)}[k]$, i.e.,

$$d_{(i)}[k] = 2^{-i} \langle f(t), \check{\psi}(2^{-i}t - k) \rangle, \quad (11)$$

where $\check{\psi}(t)$ is a dual function of $\psi(t)$. The biorthogonality condition holds across resolution levels 2^i :

$$\langle \psi(2^{-i}t - k), \check{\psi}(2^{-i}t - l) \rangle = 2^i \delta[k - l]. \quad (12)$$

The basis function $\check{\psi}(t)$ is analysis wavelet associated with the synthesis wavelet $\psi(t)$. The wavelets $\check{\psi}(t)$ and $\psi(t)$ are different in the general biorthogonal case, unless the basis functions are orthogonal. For any $i \in \mathbb{Z}$, a set of vectors $\{\psi(2^{-(i+1)}t - k)\}$ spans $\mathcal{W}_{(i+1)} \subset \mathcal{V}_{(i)}$. Thus, the wavelet coefficients $d_{(i+1)}[k]$ can be computed by discrete-time filtering of $a_{(i)}[k]$ and keeping every other sample of the output [7]. Finally, for a given signal $f(t) \in \mathcal{V}_{(0)}$ in (3), represented by its expansion coefficients $a_{(0)}[k]$ at resolution 2^0 , the wavelet decomposition is of the form

$$f(t) = \sum_{k \in \mathbb{Z}} a_{(I)}[k] \varphi(2^{-I}t - k) + \sum_{i=1}^I \sum_{k \in \mathbb{Z}} d_{(i)}[k] \psi(2^{-i}t - k). \quad (13)$$

The wavelet forward and inverse transform can be accomplished efficiently by using the perfect reconstruction filter bank described by the block diagram in Fig. 1, which is an extension of Mallat's fast wavelet algorithm [7] for non-orthogonal basis functions [27]. We denote by $\check{V}(z)$ and $\check{W}(z)$ the z -transform of the discrete-time filters in the filter bank associated with the analysis scaling and wavelet functions $\check{\varphi}(t)$ and $\check{\psi}(t)$, respectively. Analogously, $V(z)$ and $W(z)$ are the z -transform of the discrete-time filters associated with the synthesis (reconstruction) scaling and wavelet functions $\varphi(t)$ and $\psi(t)$,

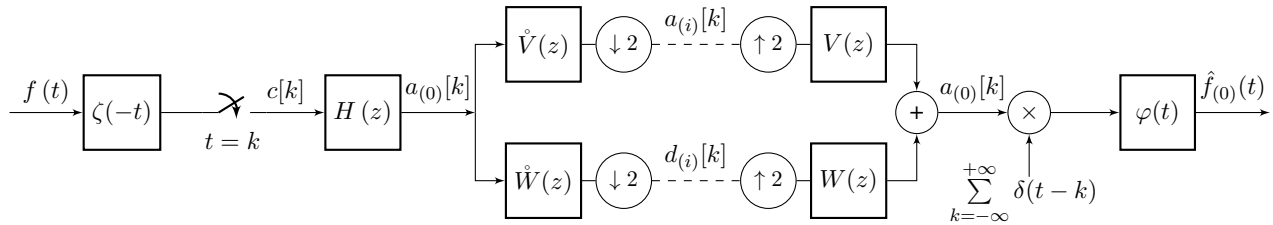


Fig. 2. Sampling and reconstruction of a signal that lies in a shift-invariant subspace with perfect reconstruction wavelet filter bank for multiresolution analysis and compression. The signal is filtered with an arbitrary sampling kernel $\zeta(t)$ before being sampled and filtered with a discrete-time correction filter $H(z)$ to obtain the expansion coefficients $a_{(0)}[k]$. Notice that the role of $\zeta(t)$ is analogous to that of an antialiasing filter in Shannon's sampling framework.

respectively. The analysis part of the block diagram in Fig. 1 is applied iteratively for $i = 0$ to $i = (I - 1)$, while keeping the wavelet coefficients for each level. The synthesis procedure is also implemented iteratively and begins with the coarsest level $i = (I - 1)$ of the pyramid. The impulse responses of the filters $\tilde{W}(z)$, $W(z)$, $\tilde{V}(z)$ and $V(z)$ depend on the choice of the scaling and wavelet basis functions based on certain desirable properties of the multiresolution analysis. The construction of a perfect reconstruction filter bank for various orthogonal and biorthogonal basis functions has been proposed in numerous papers [8], [27], [28]. For image processing, and particularly for coding applications, it is desirable to use symmetric filters with linear phase and compact support. The families of biorthogonal [29] and semi-orthogonal [30] spline wavelets [31] satisfy the desired properties, and are efficiently implemented using finite impulse response (FIR) filter banks. The scaling functions are the polynomial B-splines [6], whose integer shifts span Riesz bases.

III. GENERALIZED SAMPLING IN SHIFT-INVARIANT SPACES

Before applying the exact wavelet decomposition by using the discrete-time analysis filters, a given signal should initially be represented by appropriate approximation coefficients at resolution 2^0 . We assume that a continuous-time signal $f(t)$ lies in an SI subspace $V_{(0)}$ of L_2 and is given by (3). The generator $\varphi(t)$ forms a Riesz basis for L_2 and satisfies (4). In order to obtain a discrete-time representation, the signal is filtered with an analog prefilter and sampled uniformly at time instants k . Samples $c[k]$ in the general SI sampling scheme (see Fig. 2) can be expressed as

$$c[k] = \int_{-\infty}^{\infty} f(t)\zeta(t-k)dt \triangleq \langle f(t), \zeta(t-k) \rangle, \quad (14)$$

where $\zeta(-t)$ is the impulse response of the prefilter. Sampling in SI spaces [3]–[5] is practical and retains the shift-invariant property of the Shannon's sampling theory. In an ideal scenario, the sampling

kernel $\zeta(t)$ is orthogonal or biorthogonal to the signal generator $\varphi(t)$, which implies that $c[k] = a_{(0)}[k]$. However, in practical applications sampling is not ideal and is often imposed by a physical device. Thus, a more realistic setting is to let $\zeta(t)$ be an arbitrary sampling kernel.

Let us denote the sampled cross-correlation sequence between the sampling kernel $\zeta(t)$ and the signal generator $\varphi(t)$ with

$$r[k] = \langle \varphi(t), \zeta(t - k) \rangle. \quad (15)$$

The expression (14) of the samples $c[k]$ can be expanded to

$$\begin{aligned} c[k] &= \left\langle \sum_{l \in \mathbb{Z}} a_{(0)}[l] \varphi(t - l), \zeta(t - k) \right\rangle \\ &= \sum_{l \in \mathbb{Z}} a_{(0)}[l] \langle \varphi(t - l), \zeta(t - k) \rangle \\ &= \sum_{l \in \mathbb{Z}} a_{(0)}[l] r[k - l] = a_{(0)} * r[k], \end{aligned} \quad (16)$$

where $(*)$ is the convolution operator. Using the Fourier relations, it follows that

$$C(e^{j\omega}) = A_{(0)}(e^{j\omega})R(e^{j\omega}), \quad (17)$$

where $C(e^{j\omega})$, $A_{(0)}(e^{j\omega})$ and $R(e^{j\omega})$ are the discrete-time Fourier transforms (DTFTs) of $c[k]$, $a_{(0)}[k]$ and $r[k]$, respectively. In order to obtain $a_{(0)}[k]$, the orthogonal projection of $f(t)$ onto $\mathcal{V}_{(0)}$ can be obtained from samples $c[k]$ by filtering with a correction filter whose impulse response is given by the DTFT [3]–[5]

$$H(e^{j\omega}) = \frac{1}{R(e^{j\omega})}. \quad (18)$$

A rather mild condition on the generator $\varphi(t)$ and the sampling kernel $\zeta(t)$ should be met in order to be able to recover $a_{(0)}[k]$ from the samples [5]:

$$|R(e^{j\omega})| > \alpha, \quad (19)$$

for some constant $\alpha > 0$. In general, the Riesz basis condition (4) guarantees that (18) is well defined [4], [5]. Note that for orthogonal and biorthogonal basis functions $r[k] = \delta[k]$ and $H(e^{j\omega}) = 1$. In this case, the samples do not have to be processed by the correction filter to determine the approximation coefficients $a_{(0)}[k]$. Furthermore, when orthogonality or biorthogonality is not satisfied, an elegant SI sampling framework and an efficient implementation of the correction filter (18) is possible in B-spline function spaces [4], [32], [33]. In such function spaces, the correction filter can be determined analytically and the denominator in (18) corresponds to a concatenation of a causal and an anticausal infinite impulse response (IIR) filter with a simple expression [32]. This is due to the compact support of the polynomial

B-splines for which the cross-correlation sequence $r[k]$ has only a few nonzero symmetric entries around $k = 0$.

Once the approximation coefficients are determined, the discrete wavelet transform (DWT) described in Section II can be applied. The wavelet analysis is popular in many signal and image processing tasks, and particularly in coding applications [34] for data storage and transmission. The approximation coefficients $a_{(0)}[k]$ at resolution 2^0 can be perfectly recovered from the wavelet coefficients by repeating the process of upsampling by a factor of two and discrete-time filtering with synthesis filters. Note that $a_{(0)}[k]$ are not necessarily the pointwise values of the signal. To reconstruct the signal, $a_{(0)}[k]$ are modulated with a train of Diracs $\sum_{k \in \mathbb{Z}} \delta(t - k)$ and filtered with an analog filter whose impulse response corresponds to the generator $\varphi(t)$. The reconstruction procedure is illustrated in Fig. 2. In case when the signal $f(t)$ lies in the subspace $V_{(0)}$ spanned by $\{\varphi(t - k)\}$, the reconstruction $\hat{f}_{(0)}(t)$ is perfect, i.e., $\hat{f}_{(0)}(t) = f(t)$. Contrarily, if $f(t) \in L_2$, but does not lie specifically in $V_{(0)}$, $\hat{f}_{(0)}(t)$ is the minimum squared error approximation of the signal $f(t)$ in $V_{(0)}$. However, it is often more desirable to reconstruct the pointwise values of the signal in various resolutions than its analog representation, especially for two-dimensional signals. The pointwise values of $\hat{f}_{(0)}(t)$ is particularly efficient to obtain by using the B-spline representation [32], [33]. In this case, instead of modulation with a train of Diracs and analog filtering, the approximation coefficients $a_{(0)}[k]$ are filtered with an FIR filter that has only a few coefficients.

IV. EXTENSIONS TO HIGHER DIMENSIONS

The results in Section II and Section III can be extended to higher dimensions through the use of the tensor product, provided that the sampling is performed on the Cartesian grid [4], [7], [32]. All the formulas presented so far can be extended by considering the space variables $(u, v) \in \mathbb{R}^2$, and by replacing single summations and integrals with multiple ones. In practice, we often use separable functions of the form $\varphi(u, v) = \varphi(u)\varphi(v)$, which greatly simplify the implementation. Separability retains the one-dimensional Riesz basis condition in multiple dimensions [4]. A signal $f(u, v) \in \mathcal{V}_{(0)}^2$ has the form

$$f(u, v) = \sum_{k \in \mathbb{Z}} \sum_{l \in \mathbb{Z}} a_{(0)}[k, l] \varphi(u - k) \varphi(v - l), \quad (20)$$

where $a_{(0)}[k, l]$ are two-dimensional expansion coefficients.

In a two-dimensional wavelet decomposition, there are four types of basis functions corresponding to

a single scaling function and three wavelets:

$$\begin{aligned}
\varphi(u, v) &= \varphi(u)\varphi(v), \\
\psi_u(u, v) &= \psi(u)\varphi(v), \\
\psi_v(u, v) &= \varphi(u)\psi(v), \\
\psi_{uv}(u, v) &= \psi(u)\psi(v).
\end{aligned} \tag{21}$$

Since the corresponding wavelet decomposition is separable, it can be obtained by successive one-dimensional fast wavelet transform along the rows and columns [7], [30]. The two-dimensional wavelet decomposition is of the form

$$\begin{aligned}
f(u, v) &= \sum_{k \in \mathbb{Z}} \sum_{l \in \mathbb{Z}} a_{(I)}[k, l] \varphi(2^{-I}u - k, 2^{-I}v - l) \\
&+ \sum_{i=1}^I \sum_{k \in \mathbb{Z}} \sum_{l \in \mathbb{Z}} d_{u(i)}[k, l] \psi_u(2^{-i}u - k, 2^{-i}v - l) \\
&+ \sum_{i=1}^I \sum_{k \in \mathbb{Z}} \sum_{l \in \mathbb{Z}} d_{v(i)}[k, l] \psi_v(2^{-i}u - k, 2^{-i}v - l) \\
&+ \sum_{i=1}^I \sum_{k \in \mathbb{Z}} \sum_{l \in \mathbb{Z}} d_{uv(i)}[k, l] \psi_{uv}(2^{-i}u - k, 2^{-i}v - l).
\end{aligned} \tag{22}$$

To obtain the approximation coefficients at resolution 2^0 , $f(u, v)$ is filtered with an analog prefilter and uniformly sampled. Two-dimensional samples $c[k, l]$ can be expressed as

$$\begin{aligned}
c[k, l] &= \int_{-\infty}^{\infty} \int_{-\infty}^{\infty} f(u, v) \zeta(u - k, v - l) du dv \\
&= \sum_{m \in \mathbb{Z}} \sum_{n \in \mathbb{Z}} a_{(0)}[m, n] r[k - m] r[l - n] \\
&= (a_{(0)} ** r_k) ** r_l[k, l],
\end{aligned} \tag{23}$$

where $\zeta(u, v)$ is a separable two-dimensional sampling kernel and $(**)$ is a two-dimensional convolution operator. The convolution is separable, i.e., r_k and r_l denote row and column vectors composed of the cross-correlation sequence $r[k]$. A detailed explanation of the result in (23) is given in Appendix. It follows that all filtering operations are separable and applied successively along the coordinates.

V. SINGLE-PIXEL IMAGING VIA COMPRESSIVE SENSING IN SHIFT-INVARIANT SPACES

Sampling and reconstruction in SI spaces resembles the Nyquist-Shannon theorem. The sampling rate in the SI sampling framework is determined by a number of degrees of freedom per time unit, which is also referred to as the *rate of innovation* [9]. Signals are sampled at least at the rate of innovation

$\rho = 1/T = 1$, for $T = 1$, in order to represent $f(t)$ exactly. Note that the rate of innovation in the Nyquist-Shannon theorem corresponds to the Nyquist limit. Signals in SI spaces are often related to high rates of innovation, even though their *information rates* might be low. It is challenging to build sampling hardware that operates at a sufficient rate when the rate of innovation is high. For example, high-resolution imaging technologies in the non-visible wavelength spectrum can be impractical or very expensive to implement.

A. A Short Review of Compressive Sensing

Compressive sensing [10]–[12] is a sampling and reconstruction framework that, unlike the conventional sampling theorems, focuses on the information rate of the signal rather than its innovation rate. A signal with a low information rate can be exactly recovered from far fewer measurements (samples) in the CS framework than in the conventional sampling frameworks, even if it has a high innovation rate. The theory of CS has led to the enhancement of signal reconstructions in low-resolution imaging devices [35] and in medical devices where the full measurements are missing or not available (e.g., magnetic resonance imaging [36], computed tomography, etc.).

Compressive sensing rests on a prior that an observed signal $f(t) \in L_2$ is Q -sparse in a certain reconstruction space $\mathcal{S} = \{\xi_n(t)\}_{n=1}^N$, i.e., it is represented with at most $Q \ll N$ nonzero coefficients in a proper basis. The signal $f(t)$ is represented by coefficients $\mathbf{x} \in \mathbb{R}^N$ in the basis $\{\xi_n(t)\}_{n=1}^N$, such that $f(t) = \sum_{n=1}^N x_n \xi_n(t)$. A set of linear measurements is given by $\mathbf{y} = \mathbf{z}(f(t)) = \{z_m(t), f(t)\}_{m=1}^M$, where $M < N$. The measuring functions $z_m(t)$ are dictated by the underlying physics and assumed to be known. The forward measurement model can be converted into the discretized version $\mathbf{y} = \Theta \mathbf{x}$, where Θ is an $M \times N$ *sensing matrix* whose entries are given by $[\Theta]_{m,n} = \langle z_m(t), \xi_n(t) \rangle$. The theory of CS assumes that it is possible to reconstruct the signal from an underdetermined set of equations by restricting the expansion to no more than Q atoms in the basis $\{\xi_n(t)\}_{n=1}^N$ [10], [11]. Thus, the signal can be recovered by solving an optimization problem

$$\arg \min_{\mathbf{x} \in \mathbb{R}^N} \|\mathbf{y} - \Theta \mathbf{x}\|_{\ell_2}^2 + \lambda \|\mathbf{x}\|_{\ell_1}, \quad (24)$$

where ℓ_1 -minimization promotes sparse solutions [37]. That is, among all objects \mathbf{x} consistent with the measurements, we seek the one whose coefficient sequence has the minimum ℓ_1 norm. The regularization parameter λ in (24) sets a tradeoff between sparsity and ℓ_2 -norm error. A faithful signal recovery from $M \gtrsim 2Q$ linear measurements is possible under strict conditions on Θ , namely *restricted isometry property* (RIP) and *incoherence* [10], [38]–[40].

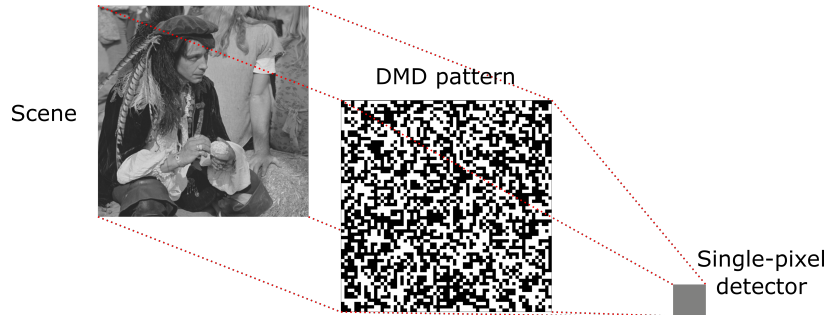


Fig. 3. **Single-Pixel Imaging.** A scene is modulated by a measurement pattern and the single-pixel detector measures the intensity of light beams that reaches its surface.

A majority of papers concerning CS rely on a discretization of the measurement process or heuristics to adopt a continuous-domain inverse problem to a finite-dimensional CS setting. A discrete measurement model of a continuous measurement process is often an approximation that can lead to bad signal reconstructions. Furthermore, it is typically assumed that the observed signal is discretized in a pixel-by-pixel basis and represented by its pointwise values. Such an assumption additionally contributes to the error related to the reconstruction of the underlying continuous-time signal. The Nyquist-Shannon model of the underlying signal may not be the best solution, since signals are often much better represented in other SI bases, such as splines [4], [5]. Recently, a framework for CS of one-dimensional signals that lie in an arbitrary SI subspace was reported in [21] and [22]. The framework links the theories of generalized sampling in SI spaces and CS, leading to an exact discretization of inherently continuous-domain inverse problems in devices specialized for CS where the sampling kernel spans an SI subspace (e.g., the random demodulator [41]).

B. Single-Pixel Compressive Imaging in SI Spaces

Single-pixel imaging modulates a scene with a sequence of spatially resolved patterns and measures the intensities of the correlations between the patterns and the scene [23], [24]. A simple illustration of single-pixel imaging is given in Fig. 3. Typically, the modulation is implemented by the DMDs, consisting of an array of individually addressable micromirrors that redirects the illumination or the light beams. The DMD is implemented as a programmable binary mask, where the value of one corresponds to full illumination of a scene (or redirection of a beam to the detector), and the value of zero means that the illumination (or the light beam) is blocked. A common approach is to use a sequence of orthogonal binary masks, e.g., the Hadamard basis, or ± 1 random Bernoulli masks, and measure the differential intensity for each pattern and its photographic negative. The single-pixel detector integrates the light photons which

fall on its surface and converts them into electrons whose number will be directly proportional to the intensity of the modulated scene.

Let us define the box function, which is also referred to as the B-spline of order zero, as:

$$b^0(t) = \begin{cases} 1, & 0 < t \leq 1 \\ 0, & \text{otherwise} \end{cases}. \quad (25)$$

The DMD measurement masks can be modeled as two-dimensional functions $\{z_m(u, v)\}_{m=1}^M$ that lie in an SI subspace \mathcal{Z} spanned by the integer shifts of a separable sampling kernel $\zeta(u, v) = b^0(u)b^0(v)$. Any spatially resolved pattern in \mathcal{Z} is given in the form

$$z_m(u, v) = \sum_{k=0}^{K-1} \sum_{l=0}^{L-1} s_m[k, l] \zeta(u - k, v - l), \quad (26)$$

where $s_m[k, l]$ are the expansion coefficients of values ± 1 , and the (K, L) pair determines the resolution of the measurement masks. By assuming that a scene model $f(u, v) \in \mathcal{V}_{(0)}^2$ is given by (20), a single measurement y_m in a single-pixel imaging system is of the form

$$\begin{aligned} y_m &= \int_{u=0}^K \int_{v=0}^L f(u, v) z_m(u, v) dudv \\ &= \int_{u=0}^K \int_{v=0}^L \left(\sum_{i \in \mathbb{Z}} \sum_{j \in \mathbb{Z}} a_{(0)}[i, j] \varphi(u - i) \varphi(v - j) \right. \\ &\quad \left. \times \sum_{k=0}^{K-1} \sum_{l=0}^{L-1} s_m[k, l] \zeta(u - k) \zeta(v - l) \right) dudv. \end{aligned} \quad (27)$$

The integration interval $[0, K] \times [0, L]$ covers the whole support of measurement masks, i.e., it covers the support of exactly $K \times L$ basis functions that span the space \mathcal{Z} . Thus, we can use the inner product notation and the results given in Appendix to express the measurement by

$$y_m = \sum_{k=0}^{K-1} \sum_{l=0}^{L-1} s_m[k, l] \sum_{i \in \mathbb{Z}} \sum_{j \in \mathbb{Z}} a_{(0)}[i, j] r[k - i] r[l - j], \quad (28)$$

where $r[k]$ is the sampled cross-correlation sequence between the one-dimensional signal generator $\varphi(t)$ and the one-dimensional sampling kernel $\zeta(t) = b^0(t)$, defined in (15). Finally, by applying (23), the measurement is given by a weighted linear combination of the samples in generalized SI sampling framework for B-spline of order zero as the sampling kernel:

$$y_m = \sum_{k=0}^{K-1} \sum_{l=0}^{L-1} s_m[k, l] c[k, l]. \quad (29)$$

Measurements $\mathbf{y} \in \mathbb{R}^M$ are given in a matrix form as:

$$\mathbf{y} = \mathbf{S}\mathbf{c}, \quad (30)$$

where \mathbf{S} is an $M \times N$ *measurement matrix*, for $N = KL$, whose rows consist of the coefficients $\{s_m[k, l]\}_{m=1}^M$. Consequently, $\mathbf{c} \in \mathbb{R}^N$ is a vector form of the samples $c[k, l]$. In single-pixel imaging, the number of measurement patterns is often $M < N$, leading to an ill-posed system of equations. The theory of CS has been extensively used in order to reconstruct the image from a reduced set of measurements. In the sequel, we will offer a solution for image reconstruction from \mathbf{y} by using CS via exact wavelet frames that intuitively complements the proposed model of the underlying signal.

C. Wavelet-Domain Sparse Reconstruction

Measurements \mathbf{y} in (30) can be expressed in the form

$$\mathbf{y} = \mathbf{S}\mathbf{R}\mathbf{a}_{(0)}, \quad (31)$$

where \mathbf{R} is a convolution matrix representing an implementation of the two-dimensional convolution with the sampled cross-correlation sequence $r[k]$, and $\mathbf{a}_{(0)}$ is a vector form of the expansion coefficients $a_{(0)}[k, l]$. If we denote the number of nonzero elements in $r[k]$ with $\Omega = \text{card}\{r[k] \mid r[k] \neq 0\}$, where card is a set cardinality, the dimension of the matrix \mathbf{R} is $N \times \tilde{N}$, for $\tilde{N} = (K + \Omega - 1)(L + \Omega - 1)$, and consequently, $\mathbf{a}_{(0)}$ is an $\tilde{N} \times 1$ vector.

Numerous papers, e.g., [16]–[19], assume that an observed signal is sparse in an alternative SI basis to the traditional Fourier basis. That is, these works use a prior that the signal can be faithfully represented with only a few nonzero expansion coefficients in a certain SI basis, such as the B-spline function space. We can exploit the same assumption in combination with our measurement model in (31) and recover the expansion coefficients $\mathbf{a}_{(0)}$ by solving (24), for $\Theta := \mathbf{S}\mathbf{R}$ and $\mathbf{x} := \mathbf{a}_{(0)}$. However, we take a different approach.

In this paper, an SI basis $\varphi(u, v)$ provides an underlying model of the observed continuous-time signal that may not be sparse when represented with the corresponding approximation coefficients $a_{(0)}[k, l]$. Instead, $a_{(0)}[k, l]$ are assumed to be sparse in a certain transform basis Ψ . While the choice of the transform basis can be arbitrary, and usually based on a signal prior [22], an intuitive option is a wavelet basis that complements the scaling function $\varphi(u, v)$. Moreover, such a pair of wavelet and scaling functions leads to an exact discretization of a continuous-domain inverse problem into a finite CS setting, where the recovered sequence corresponds to the coefficients in (22) obtained by the two-dimensional wavelet decomposition. While CS reconstruction with a wavelet-based sparsity domain has been considered previously [42]–[44], the resulting methods assume the bandlimited signal model whose discrete pointwise values $(\Psi\mathbf{x})$ are reconstructed by solving (24). Here, we use an SI signal model whose

generator is a scaling function corresponding to a specific wavelet, which leads to the reconstruction of the approximation coefficients $a_{(0)}[k, l]$ of an observed continuous-domain signal.

Consider a signal $f(u, v) \in \mathcal{V}_{(0)}^2$ given by (20), whose wavelet decomposition is of the form (22). By using discrete-time synthesis filters $v[k]$ and $w[k]$ whose z -transforms are $V(z)$ and $W(z)$ (see Fig. 1), one can construct a synthesis inverse discrete wavelet transform (IDWT) matrix $\Psi \in \mathbb{R}^{\tilde{N} \times \tilde{N}}$. The approximation coefficients $\mathbf{a}_{(0)}$ of the signal $f(u, v)$ are then given by

$$\mathbf{a}_{(0)} = \Psi \mathbf{x}, \quad (32)$$

where $\mathbf{x} = [\mathbf{a}_{(I)}^T, \mathbf{d}_{u(I)}^T, \mathbf{d}_{v(I)}^T, \mathbf{d}_{uv(I)}^T, \mathbf{d}_{u(I-1)}^T, \dots, \mathbf{d}_{uv(1)}^T]^T$ is an $\tilde{N} \times 1$ vector of wavelet decomposition coefficients. The measurements \mathbf{y} in (31) can be expanded to

$$\mathbf{y} = \mathbf{S} \mathbf{R} \Psi \mathbf{x}, \quad (33)$$

where $\Theta := \mathbf{S} \mathbf{R} \Psi$ is an $M \times \tilde{N}$ sensing matrix. We exploit the sparsity prior by using the CS framework and reconstruct the coefficients by solving an optimization problem

$$\arg \min_{\mathbf{x} \in \mathbb{R}^{\tilde{N}}} \|\mathbf{y} - \mathbf{S} \mathbf{R} \Psi \mathbf{x}\|_{\ell_2}^2 + \lambda \|\mathbf{x}\|_{\ell_1}, \quad (34)$$

where the ℓ_1 -norm regularization promotes sparse solutions.

Traditional CS is concerned with the RIP, a strict condition on a sensing matrix Θ that preserves the geometry and guarantees an exact recovery of the Q -sparse vector \mathbf{x} [10], [38]. However, over the years, the RIP has proven to be too strong an assumption, especially in practical CS applications where the exact recovery is almost impossible to achieve [40], [45]. Instead, a rather mild condition, similar to the Riesz-basis condition, is enough to be met to ensure stable recovery [46]

$$\alpha \|\mathbf{x}\|_{\ell_2}^2 \leq \|\Theta \mathbf{x}\|_{\ell_2}^2 \leq \beta \|\mathbf{x}\|_{\ell_2}^2, \quad (35)$$

for constants $0 < \alpha \leq \beta < \infty$. In this paper, the sampling kernel and the signal generator are imposed to form Riesz bases, and thus the sensing matrix $\Theta := \mathbf{S} \mathbf{R} \Psi$ satisfy the condition (35). A more convenient property of Θ that provide a concrete measure of its recovery ability is the mutual coherence. The mutual coherence of a matrix Θ , denoted $\mu(\Theta)$, measures the largest absolute correlation between any two columns θ_i, θ_j of Θ :

$$\mu(\Theta) \triangleq \max_{\substack{1 \leq i, j \leq \tilde{N} \\ i \neq j}} \frac{|\theta_i^T \theta_j|}{\|\theta_i\|_{\ell_2} \|\theta_j\|_{\ell_2}}. \quad (36)$$

Small values of the mutual coherence are preferable as they allow reconstruction of denser vectors \mathbf{x} for a fixed number of measurements M . In conventional CS, reconstruction ability can also be measured by

the coherence between the measurement and sparsity matrices. The coherence is defined as the maximal correlation between two matrices \mathbf{G} and \mathbf{H} as

$$\mu(\mathbf{G}, \mathbf{H}) \triangleq \max_{\substack{1 \leq i \leq M \\ 1 \leq j \leq N}} \frac{|g_i h_j|}{\|g_i\|_{\ell_2} \|h_j\|_{\ell_2}}, \quad (37)$$

where $\{g_i\}$ and $\{h_j\}$ are rows and columns of \mathbf{G} and \mathbf{H} , respectively. Again, small values of $\mu(\mathbf{G}, \mathbf{H})$ are desirable. Random matrices are largely incoherent with any deterministic sparsity matrix [10]. Thus, random Gaussian and Bernoulli matrices provide universal solutions to the problem of choosing an appropriate measurement matrix in the CS setting. The implementation of measurement masks with random i.i.d. values of ± 1 in single-pixel imaging is straightforward with the DMD. In the proposed framework, the sparsity matrix is Ψ , and \mathbf{S} and \mathbf{R} together form the measurement matrix, since \mathbf{R} is based on the measurement setup and the underlying signal model. The measurement matrix depends on the cross-correlation between the sampling kernel and the signal generator, which introduces a deterministic structure within the random entries of \mathbf{S} . This might increase the coherence of the sensing matrix $\Theta := \mathbf{S}\mathbf{R}\Psi$ in comparison with the coherence between the conventional pair $\mu(\mathbf{S}, \Psi)$. However, for specific SI basis functions used in the experiments, random measurement matrices are adequate choice that secures low coherence and quality reconstruction results from a small number of CS measurements.

Notice that the recovered expansion coefficients $\mathbf{a}_{(0)}$ are not necessarily the pointwise values of the signal reconstruction. They can be seen as a parametric representation of the underlying continuous-time signal obtained directly from a reduced set of linear measurements. When represented in an appropriate SI basis, the recovered signal can be processed directly in that domain without the need of transforming the coefficients into the pointwise values. B-splines are an alternative approach to the conventional bandlimited theory which offers many practical advantages in signal and image processing [6]. The underlying signal model are polynomials that are more suitable for operations like convolution or differentiation than computing discrete approximations to these mathematical constructions. Such operations are efficiently implemented with FIR filters [32], [33]. If one desires a pointwise representation of the signal, it can also be obtained by FIR filtering of the recovered coefficients $\mathbf{a}_{(0)}$, as described in Section III. Furthermore, B-splines are scaling functions of the biorthogonal wavelets [29] that are commonly used in the coding applications because of its symmetric filters with compact support. The biorthogonal wavelets are an intuitive complement of the B-spline basis functions and will be used to construct sparsity domains in the rest of the paper. However, notice that the proposed framework is not solely limited to the biorthogonal wavelets nor B-spline basis functions.

VI. ALGORITHMIC DETAILS AND IMPLEMENTATION

It is quite costly to implement random measurement matrices in practical large-scale compressive imaging applications since they require huge memory allocation, because of their unstructured nature, and necessitate many multiplications in the order of $\mathcal{O}(MN)$. There are several articles proposing methods to overcome these issues and, in this paper, we realize efficient measurement matrices by implementing the structurally-random-matrix (SRM) framework [47]. We use the matrix-free interior point method (mfIPM) [48] for solving large-scale CS optimization problems, which exploits the ability of the signal processing matrices to perform inexpensive matrix-vector multiplications that are typically in the order of $\mathcal{O}(\tilde{N})$ to $\mathcal{O}(\tilde{N} \log \tilde{N})$. Finally, the proposed CS framework is conducted on the standard test images and measurements obtained by the sensing system proposed in [49].

A. Structurally Random Measurement Matrix

A structurally random measurement matrix \mathbf{S} is defined as a product of three matrices [47]:

$$\mathbf{S} = \mathbf{D}\mathbf{F}\mathbf{P}, \quad (38)$$

where

- $\mathbf{P} \in \mathbb{R}^{N \times N}$ is a uniform random permutation matrix which scrambles the signal's sample locations.
- $\mathbf{F} \in \mathbb{R}^{N \times N}$ is a Walsh-Hadamard transform (WHT) matrix, in that SRM's entries only take values of ± 1 for compatibility with the hardware implementation.
- $\mathbf{D} \in \mathbb{R}^{M \times N}$ is a subsampling matrix which randomly picks up M rows of the matrix $\mathbf{F}\mathbf{P}$.

These matrices can be efficiently realized with their non-matrix counterparts that require only a small amount of memory storage. The costs of permutation and random subsampling are in the orders of $\mathcal{O}(N)$ and $\mathcal{O}(M)$, respectively. The fast WHT is efficiently realized with complexity in the order of $\mathcal{O}(N \log N)$ by only using the operations of additions and subtractions. The SRM performance in the CS setting is theoretically on average comparable to that of the completely random matrix, leading to a low-coherent pair of measurement and sparsity matrices [47]. A normalized WHT matrix has all the rows with zero sum of entries except for the first one, whose entries are all equal to $1/\sqrt{N}$. If the observed signal is not zero-mean, the first row should be included in the subset of selected rows to encode its average value.

B. Matrix-Free Reconstruction Algorithm

In this paper, we use mfIPM to recover an observed signal from a reduced set of linear measurements. The solver is robust and designed for sparse signal reconstruction problems that arise in the field of CS. It uses a matrix-free approach that avoids the need to explicitly formulate and store the Newton system

TABLE I
SEQUENCE $r[k]$ FOR B-SPLINE SIGNAL GENERATOR $\varphi(t)$ OF ORDER p

p	$\varphi(t)$	$r[k]$
0	$b^0(t)$	$\{\dots, 0, \underline{1}, 0, \dots\}$
1	$b^1(t)$	$\{\dots, 0, \frac{1}{8}, \underline{\frac{3}{4}}, \frac{1}{8}, 0, \dots\}$
2	$b^2(t)$	$\{\dots, 0, \frac{1}{6}, \underline{\frac{2}{3}}, \frac{1}{6}, 0, \dots\}$
3	$b^3(t)$	$\{\dots, 0, \frac{1}{384}, \frac{76}{384}, \underline{\frac{230}{384}}, \frac{76}{384}, \frac{1}{384}, 0, \dots\}$

of equations [48]. The mfIPM, as well as many other iterative ℓ_1 -minimization problem solvers, spends the majority of computational time to determine matrix-vector multiplications $\Theta \mathbf{x}$ and $\Theta^T \mathbf{x}$, where Θ is a sensing matrix. In the proposed framework, by using the notation of SRM, the problem of computing $\Theta \mathbf{x}$ is given by

$$\Theta \mathbf{x} = \mathbf{D} \mathbf{F} \mathbf{P} \mathbf{R} \Psi \mathbf{x}, \quad (39)$$

where all of the matrices have their non-matrix counterparts. Recall that \mathbf{R} is a matrix form of separable two-dimensional convolution with a cross-correlation sequence $r[k]$, and Ψ is a matrix form of the two-dimensional synthesis IDWT. The costs of the two-dimensional separable convolution and fast IDWT are in the order of $\mathcal{O}(\Omega \tilde{N})$ and $\mathcal{O}(\tilde{N})$, respectively. Notice that the number of nonzero elements Ω in the sequence $r[k]$ is rather small when the signal generator is a B-spline basis function of a low order p . B-splines of degree p are obtained by repeatedly convolving $b^0(t)$ in (25) with itself, defined recursively as $b^p(t) = b^{p-1} * b^0(t)$, for $p \in \mathbb{N}_1$. The entries of the cross-correlation sequence $r[k]$ for B-spline signal generators of orders $p = 0, \dots, 3$ are given in Table I. For a B-spline signal generator of order 0, the cross-correlation sequence $r[k] = \delta[k]$, since the sampling kernel and the generator are orthonormal. This results in $\mathbf{R} = \mathbf{I}$, where \mathbf{I} is an identity matrix, and the signal reconstruction corresponds to the conventional problem of CS type where $\Theta := \mathbf{S} \Psi$. Fast IDWT is efficiently computed by FIR filtering for synthesis spline wavelets of compact support [29], [30], whose scaling functions are B-splines.

In order to compute $\Theta^T \mathbf{x}$, we have to determine the transposes of all the matrices in (39). The transpose of the SRM is straightforward, since the normalized WHT matrix is unitary. The \mathbf{R} matrix has the transpose that is again a separable two-dimensional convolution with the same sequence $r[k]$. However, in the forward model $\Theta \mathbf{x}$, we compute only parts of the convolution that are calculated without zero-padded edges, and in the transpose, we compute the full convolution with zero-padded edges. The transpose of Ψ is implemented by using the fast DWT algorithm with the same synthesis filters used in

the IDWT. The structure of the SRM, and the low-cost convolution and DWT algorithms are exploited not only to speed up the signal reconstruction, but to even allow CS of large-scale images on a standard performance computer by saving memory space.

C. Measurement Setups for Single-Pixel Compressive Imaging

We conduct the proposed CS framework, with the algorithm described above, on a set of publicly available standard test images. The images, namely *cameraman*, *Lena*, *peppers*, *pirate*, *Barbara* and *boat*, are originally of size 512×512 . We simulate the single-pixel measurement procedure by multiplying a test image with 512×512 measurement masks of ± 1 s, such that each image pixel has its corresponding mask pixel. A single measurement y_m is obtained by summing the pixels of the image modulated with the m -th measurement mask.

Additionally, we test the proposed CS framework on real-world data obtained by the imaging system reported in [49]. The sensing system consists of a high-resolution digital projector and an off-the-shelf camera. The digital projector illuminates a scene with 256×256 masks and measurement data are acquired by the “single-pixel” camera. For low-detail scenes, good reconstruction results can be obtained from a small number of linear measurements. The \mathbf{S} matrix is an SRM obtained by using the WHT and consisting of ± 1 s. In order to implement such patterns using the projector, we separately illuminate the scene with the positive and negative components of the masks, and define the measurements as $\mathbf{y} = \mathbf{y}_{pos} - \mathbf{y}_{neg}$. This differential approach noticeably reduces the background signal noise and especially the illumination noise. However, for complex scenes with a lot of details, the number of measurements is enormous if one wants to obtain high-quality reconstruction results in 256×256 resolution. In order to efficiently and realistically simulate measurements for a high-detail scene, we use the principle of dual photography [50] and estimate light transport matrix (LTM) between the camera and the projector by following the procedure reported in [35]. We compute the high-resolution LTM between the projector of resolution 256×256 and the camera of resolution 128×128 with only a fraction of measurements and use it to calculate the light transport between the projector and an imaginary single-pixel detector at the camera location. Consequently, the single-pixel measurements are computed by $\mathbf{y}^T = \mathbf{T}\mathbf{S}^T$, where \mathbf{T} is a $1 \times N$ light transport vector and \mathbf{S} is an SRM of ± 1 s. Additionally, we use high-resolution LTMs to obtain faithful ground truths of the acquired scenes.

VII. EXPERIMENTAL RESULTS

We assess the image reconstruction quality of the proposed CS framework for various settings and compare it to the recovery ability of conventional CS. In the experiments, we use B-spline signal

generators of order $p = 0, 1, 2, 3$ that correspond to piecewise *constant*, *linear*, *quadratic* and *cubic* splines, respectively. Note that the proposed framework matches conventional single-pixel compressive imaging for B-spline of order 0. This setting is used mainly for the comparison of the frameworks. There are various complements of the B-spline scaling functions amongst spline wavelets. Here, we employ the biorthogonal wavelets reported in [29], which are very popular in image coding. The biorthogonal wavelets are denoted with $biorN_r.N_d$, where N_r and N_d are numbers of vanishing moments for the synthesis and analysis filters, respectively. A wavelet with N_r vanishing moments is orthogonal to polynomials of degree $N_r - 1$, and a synthesis scaling function of $biorN_r.N_d$ lies in an SI subspace spanned by the B-spline of order $p = N_r - 1$.

A. Numerical Experiments

First, we conduct the proposed framework on a set of standard test images. The reconstruction quality is assessed for various numbers of measurements that are computed by the simulation of single-pixel imaging described in Section VI-C. We define a measurement ratio $m_r = M/N$ as the ratio between the number of measurement masks M and the number of pixels $N = KL$ in the masks, and select ten numbers M that correspond to the ratios $m_r = 5\%, 10\%, \dots, 50\%$. Same measurement masks are used for different orders p of the B-spline basis functions in order to reject the impact of a random matrix realization on the reconstruction ability. Image reconstruction is obtained by solving the proposed ℓ_1 -minimization problem in (34). The regularization parameter λ is determined experimentally for every setting, such that it leads to the best reconstruction results in terms of the peak signal-to-noise ratio (PSNR). Reconstruction quality is assessed in terms of the PSNR in decibels and structural similarity index measure (SSIM).

Reconstruction results of the test images for various settings and the $bior2.2$ wavelets are given by the bar charts in Fig. 4. The scaling function for $bior2.2$ is the B-spline of order 1. When the approximation function $\varphi(t) = b^1(t)$, the inverse problem is exactly discretized in a sense that an input signal is decomposed by the continuous-domain wavelet functions and the recovered vector \mathbf{x} contains the coefficients given in (22). For other B-spline basis functions, the approximation coefficients $\mathbf{a}_{(0)}$ can also be assumed as sparse in the same wavelet domain. However, \mathbf{x} obtained in this way does not represent the coefficients that can be obtained by the wavelet decomposition in (22), but a certain discrete transform of the approximation sequence $\mathbf{a}_{(0)}$. The same can be applied to the $bior4.4$ wavelets whose reconstruction results for various settings are given in Fig. 5. In both Fig. 4 and Fig. 5, from the charts, it can be seen that the B-spline approximation functions $b^1(t)$, $b^2(t)$ and $b^3(t)$ achieve better results in terms of the PSNR than $b^0(t)$, which is associated with the conventional CS setting. Even though $b^0(t)$ is

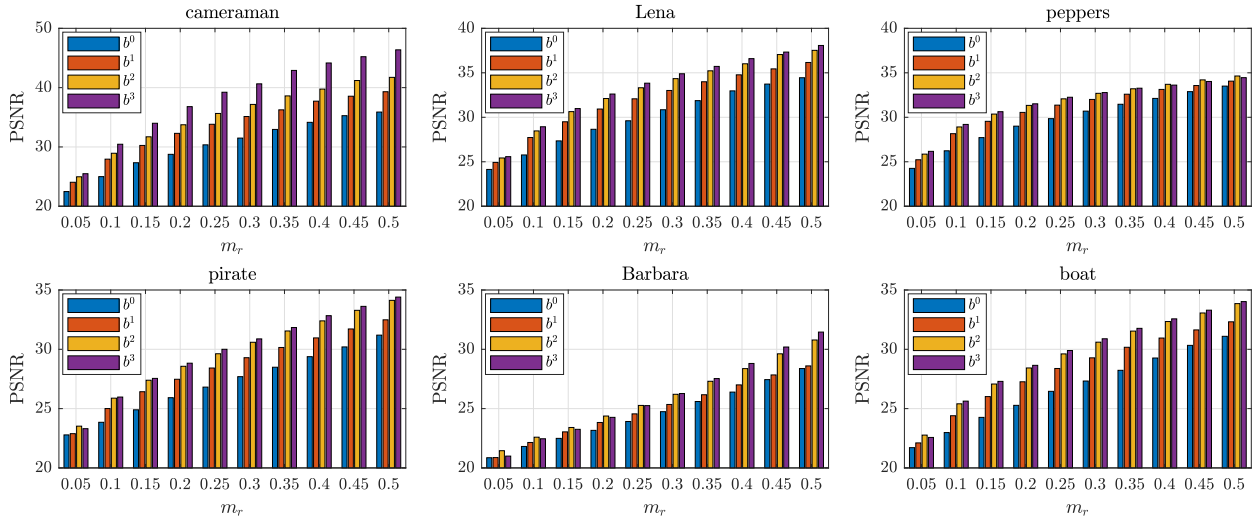


Fig. 4. **Reconstruction results for the *bior2.2* wavelets.** For a single measurement ratio m_r , there are four bars representing reconstruction results consecutively for the B-spline approximation functions of order 0 to 3. Results of the conventional method correspond to the first (blue) bar in each group.

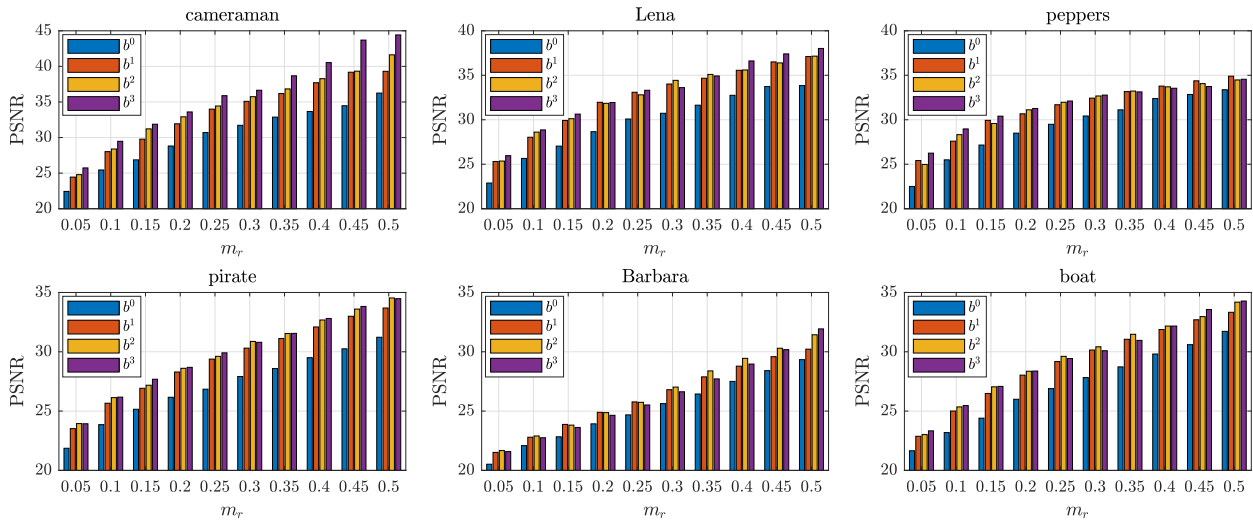


Fig. 5. **Reconstruction results for the *bior4.4* wavelets.** For a single measurement ratio m_r , there are four bars representing reconstruction results consecutively for the B-spline approximation functions of order 0 to 3. Results of the conventional method correspond to the first (blue) bar in each group.

orthogonal to the sampling kernel $\zeta(t) = b^0(t)$ and leads to the simplified CS problem where $\mathbf{R} := \mathbf{I}$, it has proven to be too coarse an approximation function in the majority single-pixel compressive imaging setups. In most settings, the $b^3(t)$ approximation function yields the best reconstruction results, achieving the same reconstruction qualities as $b^0(t)$ for approximately two times lower measurement ratios. The proposed framework achieves outstanding results for the *camaraman* when $b^3(t)$ is used, which makes

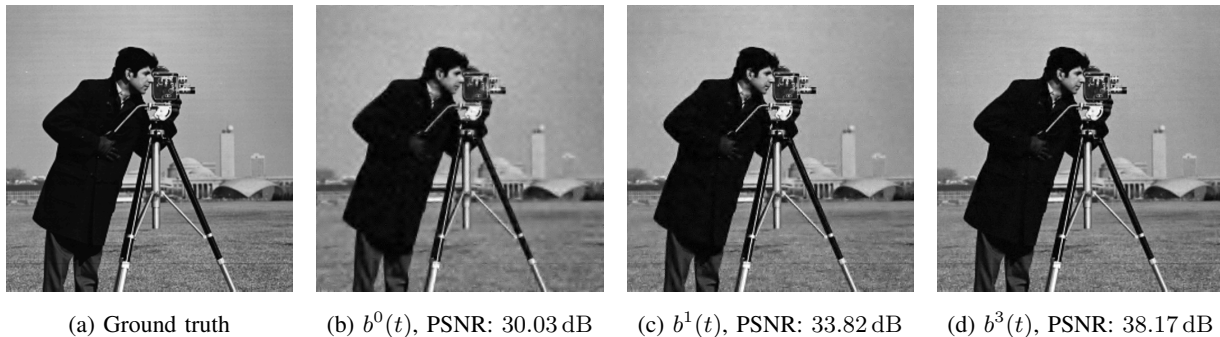


Fig. 6. **Reconstructions of the cameraman for the B-spline approximation functions of order 0, 1 and 3.** The ground truth and reconstructions are of 512×512 size. Measurement ratio is set to $m_r = 25\%$ and sparsity basis is spanned by the *bior2.2* wavelets.

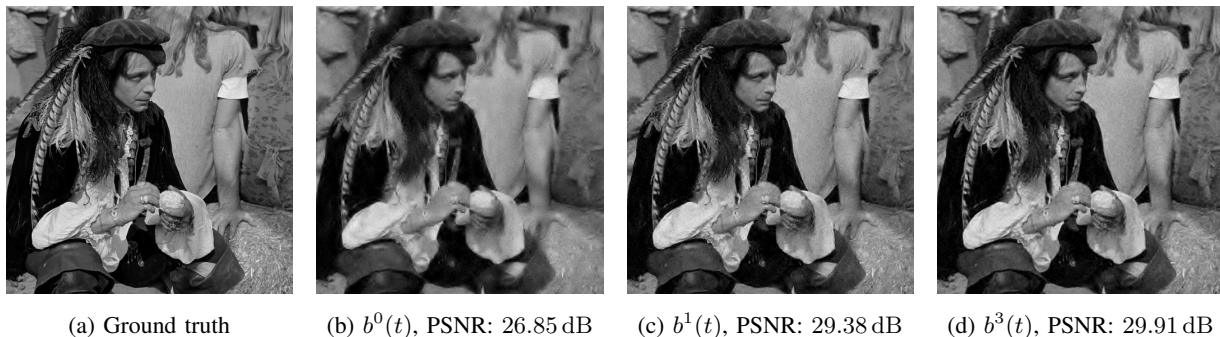


Fig. 7. **Reconstructions of the pirate for the B-spline approximation functions of order 0, 1 and 3.** The ground truth and reconstructions are of 512×512 size. Measurement ratio is set to $m_r = 25\%$ and sparsity basis is spanned by the *bior4.4* wavelets.

us suspect that its downloaded version was previously interpolated possibly with the cubic spline.

Figure 6 and Figure 7 show single image reconstructions of the *cameraman* and *pirate* for two different settings. The enhancement of the reconstruction quality for the proposed single-pixel compressive imaging framework relative to the conventional one is clearly visible.

B. Real-World Data Experiments

Figure 8 shows reconstruction results of a low-detail scene by applying the proposed CS framework on real-world data obtained by a compressive imaging system described in VI-C. The projector illuminated 8,192 patterns of 256×256 resolution and the modulated scene was captured by the “single-pixel” camera. The regularization parameter λ was tuned specifically for every setting to yield the highest SSIM. The proposed CS method outperforms the conventional one in terms of the reconstruction quality.

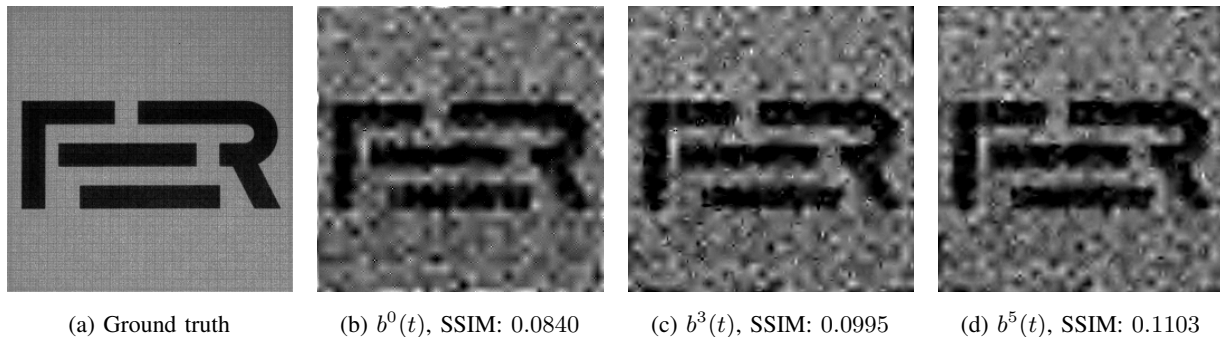


Fig. 8. **Reconstructions of a scene acquired by a real-world compressive imaging system.** B-spline approximation functions are of order 0, 3 and 5. Measurement ratio is set to $m_r = 12.5\%$. The ground truth is a *dual image* from the point of view of the projector which is obtained by dual photography.

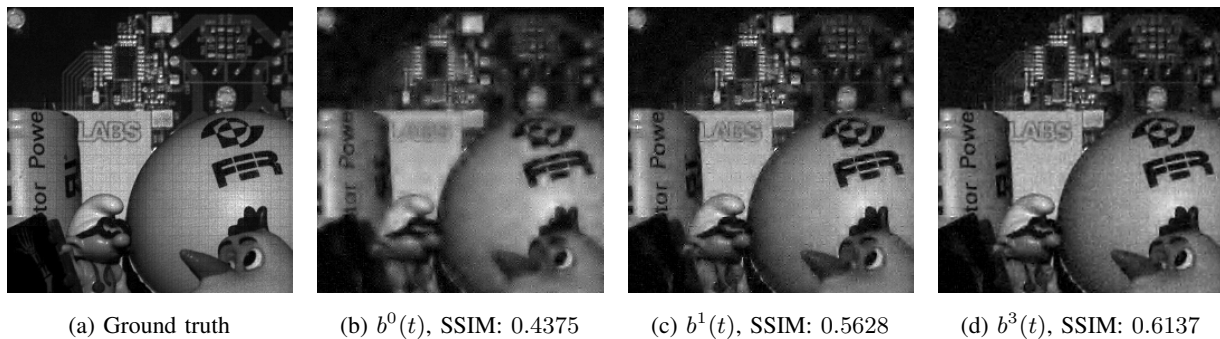


Fig. 9. **Reconstructions of a scene acquired by a dual imaging system.** B-spline approximation functions are of order 0, 1 and 3. Measurement ratio is set to $m_r = 30\%$. The ground truth is a *dual image* from the point of view of the projector which is obtained by dual photography.

For reconstruction of a high-detail scene, we used the LTM to compute the measurements of an imaginary single-pixel camera. The LTM was estimated from 1,024 CS measurements. We simulated 19,660 single-pixel measurements and reconstructed images are shown in Fig. 9. Again, λ was tuned such that it leads to the best reconstruction results for every setting in terms of the SSIM. Both the B-spline representations of order 1 and 3 yield high-quality reconstruction results and overachieve the conventional B-spline of order 0. In all settings in both Fig. 8 and Fig. 9, we used the *bior2.2* wavelets.

VIII. RELATED WORK

In [16] and [17], analog signals are assumed to lie in unions of SI subspaces. An SI signal model is used to exactly discretize a continuous-domain inverse problem and to induce sparsity which is modeled by assuming that only a few out of all generators are active. Compressive sensing is employed in order to reduce the number of analog filters preceding sampling at the rate of innovation. The framework can

be extended to a special case of sampling of analog signals that lie in an SI space spanned by a single generator. However, this leads to a signal model whose expansion coefficients are assumed sparse in a sense that only a few of them are nonzero. The authors propose analog filters with sampling kernels that are linear combinations of the shifts of a function biorthogonal to a generator. Such filters may be quite difficult to implement in hardware, especially in imaging modalities, and are often approximated which introduces errors in the system.

Unser et al. [18] introduce a method for solving continuous-domain inverse problems with sparse spline solutions by using the total-variation regularization. As demonstrated in [19] and [20], which are papers that rely on the main results of [18], the grid-based discretization strategies lead to convex optimization problems that can be efficiently solved. The framework exploits an assumption that the signal has a low innovation rate, i.e., the innovation occurs only at a few locations out of all on some predefined grid. The signal model can be interpreted as a spline that has a small number of nonzero expansion coefficients.

In [22], the authors propose a SI signal model for an exact discretization of one-dimensional continuous-time inverse problems. The underlying signal is assumed to lie in a single SI subspace, but contrarily to the works mentioned above, the SI model does not induce sparsity. Instead, it introduces an alternative approach to the Nyquist-Shannon signal model, which is conventionally assumed in CS. In order to employ CS, the authors assume that the expansion coefficients, which are not necessarily pointwise values of the signal, are sparse in a certain discrete transform domain. The paper reinterprets the random demodulator [41] as a system for CS of signals in more general class of SI subspaces. The emphasis is put on the generalization of the system to arbitrary sampling kernels and conditions on the boundaries of integration intervals.

In this paper, we use an SI signal model to recast a two-dimensional continuous-domain inverse problem as a finite dimensional CS problem in an exact way. The proposed framework fits perfectly to the concept of single-pixel imaging. The emphasis is put on the multiresolution analysis that yields complement sparsity bases to the B-spline representation functions. When a representation function corresponds to a certain wavelet scaling function, the problem of signal decomposition is exact. Additionally, we offer an efficient implementation that can be used for reconstruction of large-scale images. Finally, extensive experiments were conducted on the standard test images and data obtained by a real acquisition system.

IX. DISCUSSION AND CONCLUSION

We proposed a novel framework for single-pixel imaging via CS. The paper successfully links the theories of CS and generalized sampling in SI spaces. The SI property of the underlying continuous-domain signal model leads to an exact discretization of the ill-posed inverse problem. Such a model

perfectly fits the CS paradigm, where the ℓ_1 -norm regularization promotes sparse solutions. In order to induce sparsity, we exploit the assumption that the expansion coefficients of the underlying signal are sparse in a certain sparsity domain.

Traditionally, the signal is assumed to be bandlimited, i.e., the underlying signal model rests on the Nyquist-Shannon principles. However, it is just an approximation in the case of single-pixel compressive imaging. We showed that the conventional problem is an exact discretization when the underlying model is B-spline of order 0. In this paper, we proposed a CS framework for a single-pixel camera that uses an arbitrary SI signal model and showed that B-splines of higher orders lead to efficient implementations and better reconstruction results in comparison to the conventional setting. Furthermore, directly recovered B-spline signal representation is an alternative approach whose polynomial interpretation offers many practical advantages in image processing applications.

The fact that the B-splines correspond to scaling functions in spline wavelet frames has led us to use the biorthogonal wavelets as sparsity-inducing dictionaries. We proved that the coefficients recovered by solving the CS optimization problem are wavelet coefficients corresponding to the orthogonal projections of the signal onto the continuous-domain analysis wavelet functions when the B-spline representation function is equal to the scaling function. However, the extensive experimental results have shown that, in general, higher orders of B-spline representation functions yield better reconstructions even when the scaling function corresponds to a B-spline of low order. That is, it is more important to choose a proper underlying signal model than to match the representation function with the scaling function of a frame.

We offered an efficient matrix-free implementation of the proposed framework and conducted it on synthetic and real-world measurement data. The experiments have shown that the proposed framework overachieves the conventional one in both noise-free synthetic and noisy real-world scenarios.

APPENDIX

Samples $c[k, l]$ in a general SI sampling framework for the separable two-dimensional sampling kernel $\zeta(u, v)$ and signal generator $\varphi(u, v)$ are given by

$$\begin{aligned}
c[k, l] &= \int_{-\infty}^{\infty} \int_{-\infty}^{\infty} f(u, v) \zeta(u - k, v - l) du dv \\
&= \int_{-\infty}^{\infty} \int_{-\infty}^{\infty} \left(\sum_{m \in \mathbb{Z}} \sum_{n \in \mathbb{Z}} a_{(0)}[m, n] \varphi(u - m) \varphi(v - n) \right. \\
&\quad \left. \times \zeta(u - k) \zeta(v - l) \right) du dv \\
&= \sum_{m \in \mathbb{Z}} \sum_{n \in \mathbb{Z}} a_{(0)}[m, n] \int_{-\infty}^{\infty} \varphi(u - m) \zeta(u - k) du \\
&\quad \times \int_{-\infty}^{\infty} \varphi(v - n) \zeta(v - l) dv.
\end{aligned} \tag{40}$$

By using the inner product definition in (2), (40) becomes

$$\begin{aligned}
c[k, l] &= \sum_{m \in \mathbb{Z}} \sum_{n \in \mathbb{Z}} a_{(0)}[m, n] \langle \varphi(u - m), \zeta(u - k) \rangle \\
&\quad \times \langle \varphi(v - n), \zeta(v - l) \rangle.
\end{aligned} \tag{41}$$

The inner products of the basis functions are the sampled cross-correlation sequences defined in (15). Thus, the samples $c[k, l]$ are given by the separable two-dimensional convolution between the expansion coefficients $a_{(0)}[k, l]$ and the sampled cross-correlation sequence $r[k]$ in (23).

ACKNOWLEDGMENT

The authors would like to thank Ivan Ralašić for providing codes for the off-the-shelf compressive imaging system and fruitful discussion on the system parameters and geometry, and to Professor Sven Lončarić for lending an industrial camera and a projector for the experiments.

REFERENCES

- [1] H. Nyquist, "Certain topics in telegraph transmission theory," *Trans. AIEE*, vol. 47, no. 2, pp. 617–644, Apr. 1928.
- [2] C. E. Shannon, "Communication in the presence of noise," *Proc. IRE*, vol. 37, no. 1, pp. 10–21, Jan. 1949.
- [3] M. Unser and A. Aldroubi, "A general sampling theory for nonideal acquisition devices," *IEEE Trans. Signal Process.*, vol. 42, no. 11, pp. 2915–2925, 1994.
- [4] M. Unser, "Sampling-50 years after Shannon," *Proc. IEEE*, vol. 88, no. 4, pp. 569–587, Apr. 2000.

- [5] Y. C. Eldar and T. Michaeli, “Beyond bandlimited sampling,” *IEEE Signal Process. Mag.*, vol. 26, no. 3, pp. 48–68, May 2009.
- [6] M. Unser, “Splines: A perfect fit for signal and image processing,” *IEEE Signal Process. Mag.*, vol. 16, no. 6, pp. 22–38, 1999.
- [7] S. Mallat, “A theory for multiresolution signal decomposition: The wavelet representation,” *IEEE Trans. Pattern Anal. Mach. Intell.*, vol. 11, no. 7, pp. 674–693, Jul. 1989.
- [8] I. Daubechies, “The wavelet transform, time-frequency localization and signal analysis,” *IEEE Trans. Inf. Theory*, vol. 36, no. 5, pp. 961–1005, 1990.
- [9] M. Vetterli, P. Marziliano, and T. Blu, “Sampling signals with finite rate of innovation,” *IEEE Trans. Signal Process.*, vol. 50, no. 6, pp. 1417–1428, Jun. 2002.
- [10] E. Candès, J. Romberg, and T. Tao, “Robust uncertainty principles: Exact signal reconstruction from highly incomplete frequency information,” *IEEE Trans. Inf. Theory*, vol. 52, no. 2, pp. 489–509, Feb. 2006.
- [11] D. Donoho, “Compressed sensing,” *IEEE Trans. Inf. Theory*, vol. 52, no. 4, pp. 1289–1306, Apr. 2006.
- [12] S. Foucart and H. Rauhut, *A Mathematical Introduction to Compressive Sensing*. Springer New York, 2013.
- [13] M. Mishali, Y. C. Eldar, and A. J. Elron, “Xampling: Signal acquisition and processing in union of subspaces,” *IEEE Trans. Signal Process.*, vol. 59, no. 10, pp. 4719–4734, Oct. 2011.
- [14] B. Adcock and A. C. Hansen, “Generalized sampling and infinite-dimensional compressed sensing,” *Found. Comput. Math.*, vol. 16, no. 5, pp. 1263–1323, Aug. 2016.
- [15] B. Adcock, “Infinite-dimensional compressed sensing and function interpolation,” *Found. Comput. Math.*, vol. 18, no. 3, pp. 661–701, Apr. 2018.
- [16] Y. C. Eldar, “Compressed sensing of analog signals in shift-invariant spaces,” *IEEE Trans. Signal Process.*, vol. 57, no. 8, pp. 2986–2997, Aug. 2009.
- [17] Y. C. Eldar and M. Mishali, “Robust recovery of signals from a structured union of subspaces,” *IEEE Trans. Inf. Theory*, vol. 55, no. 11, pp. 5302–5316, Nov. 2009.
- [18] M. Unser, J. Fageot, and J. P. Ward, “Splines are universal solutions of linear inverse problems with generalized TV regularization,” *SIAM Rev.*, vol. 59, no. 4, pp. 769–793, Jan. 2017.
- [19] T. Debarre, J. Fageot, H. Gupta, and M. Unser, “B-spline-based exact discretization of continuous-domain inverse problems with generalized TV regularization,” *IEEE Trans. Inf. Theory*, vol. 65, no. 7, pp. 4457–4470, Jul. 2019.
- [20] T. Debarre, S. Aziznejad, and M. Unser, “Hybrid-spline dictionaries for continuous-domain inverse problems,” *IEEE Trans. Signal Process.*, vol. 67, no. 22, pp. 5824–5836, Nov. 2019.
- [21] T. Vlačić and D. Seršić, “Sub-Nyquist sampling in shift-invariant spaces,” in *2020 28th European Signal Processing Conference (EUSIPCO)*, Jan. 2021, pp. 2284–2288.
- [22] —, “Sampling and reconstruction of sparse signals in shift-invariant spaces: Generalized Shannon’s theorem meets compressive sensing,” *ArXiv:2010.15618*, Oct. 2020, submitted for publication.
- [23] M. F. Duarte *et al.*, “Single-pixel imaging via compressive sampling,” *IEEE Signal Process. Mag.*, vol. 25, no. 2, pp. 83–91, Mar. 2008.
- [24] G. M. Gibson, S. D. Johnson, and M. J. Padgett, “Single-pixel imaging 12 years on: a review,” *Opt. Express*, vol. 28, no. 19, p. 28190, Sep. 2020.
- [25] O. Christensen, *An Introduction to Frames and Riesz Bases*. Birkhäuser Boston, 2003.
- [26] M. Unser, A. Aldroubi, and M. Eden, “The L_2 -polynomial spline pyramid,” *IEEE Trans. Pattern Anal. Mach. Intell.*, vol. 15, no. 4, pp. 364–379, Apr. 1993.

- [27] M. Vetterli and C. Herley, “Wavelets and filter banks: Theory and design,” *IEEE Trans. Signal Process.*, vol. 40, no. 9, pp. 2207–2232, Sep. 1992.
- [28] I. Daubechies, “Orthonormal bases of compactly supported wavelets,” *Commun. Pure Appl. Math.*, vol. 41, no. 7, pp. 909–996, Oct. 1988.
- [29] A. Cohen, I. Daubechies, and J.-C. Feauveau, “Biorthogonal bases of compactly supported wavelets,” *Commun. Pure Appl. Math.*, vol. 45, no. 5, pp. 485–560, Jun. 1992.
- [30] M. Unser, A. Aldroubi, and M. Eden, “A family of polynomial spline wavelet transforms,” *Signal Process.*, vol. 30, no. 2, pp. 141–162, Jan. 1993.
- [31] M. A. Unser, “Ten good reasons for using spline wavelets,” in *Wavelet Applications in Signal and Image Processing V*, Oct. 1997.
- [32] M. Unser, A. Aldroubi, and M. Eden, “B-spline signal processing. I. Theory,” *IEEE Trans. Signal Process.*, vol. 41, no. 2, pp. 821–833, 1993.
- [33] —, “B-spline signal processing. II. Efficiency design and applications,” *IEEE Trans. Signal Process.*, vol. 41, no. 2, pp. 834–848, 1993.
- [34] B. Usevitch, “A tutorial on modern lossy wavelet image compression: Foundations of JPEG 2000,” *IEEE Sig. Process. Mag.*, vol. 18, no. 5, pp. 22–35, 2001.
- [35] I. Ralasic, M. Donlic, and D. Sersic, “Dual imaging—Can virtual be better than real?” *IEEE Access*, vol. 8, pp. 40 246–40 260, 2020.
- [36] M. Lustig, D. Donoho, and J. M. Pauly, “Sparse MRI: The application of compressed sensing for rapid MR imaging,” *Magn. Reson. Med.*, vol. 58, no. 6, pp. 1182–1195, 2007.
- [37] D. L. Donoho, “For most large underdetermined systems of linear equations the minimal ℓ_1 -norm solution is also the sparsest solution,” *Commun. Pure Appl. Math.*, vol. 59, no. 6, pp. 797–829, 2006.
- [38] E. J. Candès, “The restricted isometry property and its implications for compressed sensing,” *Comptes Rendus Math.*, vol. 346, no. 9–10, pp. 589–592, May 2008.
- [39] B. Roman, A. Hansen, and B. Adcock, “On asymptotic structure in compressed sensing,” *ArXiv:1406.4178*, 2014.
- [40] B. Adcock, A. C. Hansen, C. Poon, and B. Roman, “Breaking the coherence barrier: A new theory for compressed sensing,” *Forum Math. Sigma*, vol. 5, 2017.
- [41] J. A. Tropp, J. N. Laska, M. F. Duarte, J. K. Romberg, and R. G. Baraniuk, “Beyond nyquist: Efficient sampling of sparse bandlimited signals,” *IEEE Trans. Inf. Theory*, vol. 56, no. 1, pp. 520–544, Jan. 2010.
- [42] L. He and L. Carin, “Exploiting structure in wavelet-based Bayesian compressive sensing,” *IEEE Trans. Signal Process.*, vol. 57, no. 9, pp. 3488–3497, Sep. 2009.
- [43] R. G. Baraniuk, V. Cevher, M. F. Duarte, and C. Hegde, “Model-based compressive sensing,” *IEEE Trans. Inf. Theory*, vol. 56, no. 4, pp. 1982–2001, Apr. 2010.
- [44] M. F. Duarte and R. G. Baraniuk, “Compressive sensing with biorthogonal wavelets via structured sparsity,” in *Workshop on Signal Processing with Adaptive Sparse Representations (SPARS)*, 2011.
- [45] A. Bastounis and A. C. Hansen, “On the absence of the RIP in real-world applications of compressed sensing and the RIP in levels,” *ArXiv:1411.4449*, 2015.
- [46] Y. C. Eldar, “Compressed sensing,” in *Sampling Theory*. Cambridge University Press, 2015, ch. 11, pp. 392–474.
- [47] T. T. Do, L. Gan, N. H. Nguyen, and T. D. Tran, “Fast and efficient compressive sensing using structurally random matrices,” *IEEE Trans. Signal Process.*, vol. 60, no. 1, pp. 139–154, Jan. 2012.

- [48] K. Fountoulakis, J. Gondzio, and P. Zhlobich, “Matrix-free interior point method for compressed sensing problems,” *Math. Program. Comput.*, vol. 6, no. 1, pp. 1–31, Dec. 2013.
- [49] I. Ralašić, D. Seršić, and D. Petrinović, “Off-the-shelf measurement setup for compressive imaging,” *IEEE Trans. Instrum. Meas.*, vol. 68, no. 2, pp. 502–511, Feb. 2019.
- [50] P. Sen *et al.*, “Dual photography,” *ACM Trans. Graph.*, vol. 24, no. 3, pp. 745–755, Jul. 2005.